



Obrabotka metallov -

Metal Working and Material Science

Journal homepage: http://journals.nstu.ru/obrabotka_metallov



Relationship between microstructure and impact toughness of weld metals in pipe high-strength low-alloy steels (research review)

Yulia Karlina^{1, a, *}, Roman Kononenko^{2, b}, Vladimir Ivancivsky^{3, c}, Maksim Popov^{2, d},
 Fedor Derjugin^{2, e}, Vladislav Byankin^{2, f}

¹ National Research Moscow State University of Civil Engineering, 26 Yaroslavskoe Shosse, Moscow, 129337, Russian Federation

² Irkutsk National Research Technical University, 83 Lermontova str., Irkutsk, 664074, Russian Federation

³ Novosibirsk State Technical University, 20 Prospekt K. Marksa, Novosibirsk, 630073, Russian Federation

^a  <https://orcid.org/0000-0001-6519-561X>,  jul.karlina@gmail.com; ^b  <https://orcid.org/0009-0001-5900-065X>,  istu_politeh@mail.ru;

^c  <https://orcid.org/0000-0001-9244-225X>,  ivancivskij@corp.nstu.ru; ^d  <https://orcid.org/0000-0003-2387-9620>,  popovma.kvantum@gmail.com;

^e  <https://orcid.org/0009-0004-4677-3970>,  deryugin040301@yandex.ru; ^f  <https://orcid.org/0009-0007-0488-2724>,  borck3420@gmail.com

ARTICLE INFO

Article history:

Received: 19 September 2023

Revised: 21 October 2023

Accepted: 16 January 2024

Available online: 15 March 2024

Keywords:

Steel
 Ferrite
 Perlite
 Bainite
 Martensite
 Impact toughness
 Fracture
 Hybrid laser welding
 Standards

Acknowledgements

Research was partially conducted at core facility “Structure, mechanical and physical properties of materials”.

ABSTRACT

Introduction. The modern pipeline industry requires the development of materials of high strength and toughness for the production of steels for oil and gas pipelines. Changes in steel production and rolling technologies have become a challenge for developers of welding materials and joining technologies. This problem is more critical for strength levels above 830 MPa, where there are no special rules for the approval of welding consumables. **Research methods.** The failure of stainless steel pipeline welds is becoming a serious problem in the pipeline industry. Multiphase microstructures containing acicular ferrite or an acicular ferrite-dominated phase exhibit good complex properties in HSLA steels. This paper focuses on the results obtained using modern methods of scanning electron microscopy for microstructural analysis, backscattered electrons (BSE) for electron channel contrast imaging (ECCI) and orientation microscopy based on electron backscatter diffraction (ORM), as well as characteristic X-rays for compositional analysis using X-beam spectroscopy (XEDS) and secondary electrons (SE) to observe surface morphology. **Results and discussion.** This paper analyzes the characteristics of the microstructure of the weld and its relationship with impact toughness. It is shown that predicting impact toughness based on the microstructural characteristics of steel weld metals is complicated due to the large number of parameters involved. This requires an optimal microstructure of the steel. Satisfactory microstructure depends on several factors, such as chemical composition, hot work processing, and accelerated cooling. Alloying elements have a complex effect on the properties of steel, and alloying additives commonly added to the steel composition include Mn, Mo, Ti, Nb and V. From a metallurgical point of view, the choice of alloying elements and the metallurgical process can greatly influence the resulting microstructure. A longer cooling time tend to improve the toughness and reduce the mechanical strength of weld deposits on high-strength steels. Welding thermal cycles cause significant changes in the mechanical properties of the base material. The analysis showed that impact toughness strongly depends on the microstructure of the multi-pass weld of the material under study, which contains several sources of heterogeneity, such as interdendritic segregation, and the effective grain size can also be a significant factor explaining large deviations in local impact toughness values. Acicular ferrite nucleated in intragranular inclusions has been shown to produce a fine-grained interlocking arrangement of ferrite plates providing high tensile strength and excellent toughness, and is therefore a desirable microstructural constituent in C-Mn steel weld metals. At the same time, discussion regarding the relationship between acicular ferrite and toughness is very complex and still open at present. Relating impact toughness to acicular ferrite, taking into account the top bead, is not a reliable procedure, even for single-pass deposit welding. Impact strength depends on several factors, and the strong effect of acicular ferrite is generally recognized due to its fine-grained interlocking structure, which prevents the propagation of brittle cracks by cleavage. The large-angle boundaries and high dislocation density of acicular ferrite provide high strength and toughness. However, for the same amount of acicular ferrite, different viscosity values may be observed depending on the content of microalloying elements in the steel. An analysis of the results of various studies showed that other factors also affect the impact strength. For example, microphases present along the Charpy-V notch are critical for the toughness of weld metals. The combination of OM, SEM and EBSD techniques provides an interesting method for metallographic investigation of the refined metal microstructure of stainless steel pipeline welds. **Conclusion.** This review reports the most representative study regarding the microstructural factor in the weld of pipe steels. It includes a summary of the most important process variables, material properties, regulatory guidelines, and microstructure characteristics and mechanical properties of the joints. This review is intended to benefit readers from a variety of backgrounds, from non-welding or materials scientists to various industrial application specialists and researchers.

For citation: Karlina Y.I., Kononenko R.V., Ivancivsky V.V., Popov M.A., Derjugin F.F., Byankin V.E. Relationship between microstructure and impact toughness of weld metals in pipe high-strength low-alloy steels (research review). *Obrabotka metallov (tekhnologiya, oborudovanie, instrumenty)* = *Metal Working and Material Science*, 2024, vol. 26, no. 1, pp. 129–154. DOI: 10.17212/1994-6309-2024-26.1-129-154. (In Russian).

* Corresponding author

Karlina Yulia I., Ph.D. (Engineering), Research Associate
 National Research Moscow State Construction University,
 Yaroslavskoe shosse, 26,
 129337, Moscow, Russian Federation
 Tel.: +7 914 879-85-05, e-mail: jul.karlina@gmail.com

Introduction

In the review [1], the features of the chemical composition of pipe steels, welding methods, and regulatory documents regulating mechanical properties are considered. In this paper we will consider the characteristics of the microstructure of welded joints.

Increasing the yield strength is known to increase the loading capacity and reduce the transportation costs. Thus, high strength combined with high toughness and formability are the main requirements in the steel industry for pipelines [2–10]. The addition of micro-alloying elements such as *Nb*, *V*, *Ti* and *Mo*, coupled with advanced thermo-mechanical control process (*TMCP*) technology, can provide an excellent combination of strength and toughness [2, 3]. Microalloying elements such as *Ti* and *Nb* form finely dispersed carbide and carbonitride precipitates during *TMCP* of high-quality pipeline steels, which increase the strength of the steel. It has been established that fairly homogeneous dispersed particles containing *Nb*, *Ti* and *V* effectively inhibit the growth of austenite grains [11–15]. Besides, the additions of *Mo*, *Nb* and *Cu* contributed to the formation of a bainite microstructure [11–16].

The effect of carbide size on fracture may be indirectly related to grain size. The authors of [3, 11, 12] noted that the largest size of carbides in the microstructure is proportional to the size of the ferrite grain in annealed or normalized steels. Grain size is important even when cracks are initiated by pearlite particles or colonies, [11, 12] because the grains around the fracture source can control crack propagation [1–3]. Larger grains, if present around the source of the spall, encourage the nucleated crack to grow beyond the critical size required for unstable propagation before it can be blocked by the grain boundary. As a result, failure occurs at a lower stress than required when smaller grains are present around the start of the fracture. Observations such as the presence of non-propagating ferrite grain-sized cracks on the fracture surface [11], large cleavage facets at the crack nucleation (larger than the average facet size) [12–15], and better correlation between fracture stress and largest grain size (and not the average grain size) in fractured ferritic-pearlite steel specimens [17–25] is important in the initiation and propagation of cleavage cracks.

At the same time, it should be understood that within the volume of a structural material, spatial inhomogeneities can arise in various forms, such as a non-uniform distribution of non-metallic inclusions and precipitates, a spatial distribution of pearlite and ferrite, a mixed (fine- and coarse-grained) granular structure (or crystallographic texture) [1–3]. The authors [3, 11, 12, 24, 25] concluded that spatial heterogeneity in any form can lead to a wider than usual scatter of fracture toughness results, depending on the local microstructure sampled at the “critical distance” (at where the local tensile stress exceeds the cleavage stress). Fracture stress [25] in front of the notch root. The grain size in steels can be irregular, and in some *Nb-V* steel plates subjected to thermo-mechanical control process (*TMCP*), a bimodal ferrite grain size distribution has been reported (coarse grains present in a matrix of fine grains) [11]. Therefore, depending on whether the grains are large or small at the root of the notch, the fracture stress values for a bimodal ferrite structure may differ. Understanding the spread of *Charpy* energy values for steels after *TMCP* is very important from an industrial point of view. However, it is scientifically difficult to study the effect of particle size distribution on impact strength using *Charpy* tests. *Charpy* tests often produce complex fracture surfaces that make it difficult to identify the original location of the onset of cleavage [11, 25–28]. For example, works [11, 12] have shown that in a blunt notch test, if a coarse grain band is present in the active area just before the root of the notch, the coarse grains initiate spalling, which results in low shear failure stress. However, if large grains are absent at the root of the notch, small grains initiate spalling and fracture stress values are higher. Similarly, in the *Charpy* impact transition (*IT*) region, the magnitude of the plastic fracture area depends on the location of the coarse grain band relative to the root of the notch. If the coarse grain band is located close to the base of the cut, cleavage failure begins at that location, resulting in low impact energy. However, if the coarse grain strip is located far from the base of the notch, a ductile crack will propagate first, absorbing higher impact energy.

In addition to the above, the works [3, 11, 12, 15–19] show that the addition of a large amount of micro-alloying elements poses a serious problem for the weldability of pipeline steel due to the increased equivalent carbon content (C_{eq} according to the Russian standard), especially such elements as *Ni*, *V*, *Cr*, *Mo* and *Cu* [2, 4, 11–28].

Research methods

Predicting impact toughness based on the microstructural characteristics of weld metals is difficult due to the large number of parameters involved [1, 11–18]. The common practice of relating impact toughness to the microstructure of the last bead of a multi-pass weld turned out to be unsatisfactory since the amount of acicular ferrite, the most desirable component, may not always make the main contribution to the impact toughness [20–32]. Parameters such as the recrystallized fraction, the presence of micro-phases and inclusions can also play an important role [32–36, 37–48]. Thus, in order to take into account the influence of all these parameters, the method [38, 39] proposed by the *International Institute of Welding (IIW)* is not comprehensive enough and therefore additional methods are needed. This situation is more relevant for high-strength steel weldments where very fine microstructures cannot be clearly identified, resulting in incorrect microstructure identification. The use of scanning electron microscopy as an auxiliary method to optical microscopy has been successfully used for many decades to study *C-Mn* and low-alloy metal welds, mainly in the assessment of refined microstructure. Recently [49–61], in addition to the previously mentioned methods, electron backscatter diffraction (*EBS*D) has also been used to provide a more efficient analytical procedure. This method, which provides valuable grain boundary information, is useful for refined microstructures to confirm constituents such as acicular ferrite, bainite and martensite.

The mechanical properties of high-strength low-alloy pipe steels largely depend on its complex microstructure. However, the precise quantitative influence of individual microstructural elements (e.g., dislocations, grain boundaries, phase boundaries, volume fractions of the corresponding microstructure components, phase types, dispersion and shape of martensite islands, etc.) [2, 3, 11] is usually not easy to measure with traditional optical microscopy methods. Thus, it is a general question how to obtain quantitative values of the types and quantities of these different microstructural components and its topological features. Various electron diffraction techniques, mainly used in scanning electron microscopy (*SEM*), are capable of providing comprehensive answers to these questions. Modern scanning electron microscopes with thermal field emission guns, various sensitive detectors and flexible stages are extremely versatile tools for detailed and quantitative analysis of the microstructure of bulk materials' specimens with high resolution, with large statistics, in 2D and 3D, as well as provide the opportunity to implement various types of field observations. The most important signals to be detected for microstructural analysis are backscattered electrons (*BSE*) for electron channel contrast imaging (*ECCI*) and orientation microscopy based on electron backscatter diffraction (*ORM*), as well as characteristic X-rays for compositional analysis using X-beam spectroscopy (*XEDS*) and secondary electron (*SE*) to observe surface morphology.

The purpose of the work is to evaluate the various microstructures of metal welds of *C-Mn* and high-strength steels based on the analysis of various studies carried out by optical microscopy, scanning electron microscopy and *EBS*D methods, taking into account the influence of recrystallization in multi-pass welds, microstructural components, micro-phases, and inclusion. The objective of this analysis is to establish the relationship between the microstructure and toughness of some experimental results obtained over the past decades for weld metals with tensile strength from 400 to 1,000 MPa. The analysis was carried out using the methodology proposed in [32], to verify its effectiveness and explanation impact toughness behavior.

Research results of several authors and discussion

Influence of carbon equivalent on tensile strength and impact toughness of weld metals

Figure 1 shows the effect of carbon equivalent on the strength and toughness of the weld metal from the review work [32]. It was shown in [32] that C_{eq} has a high dependency on the tensile strength of the weld metals (figure 1, *a*), and some studies have shown an almost linear increase in the ultimate strength of the weld metal with increasing C_{eq} .

It can be seen that with an increase in the strength of the metal, a high scatter of values is observed, which may be due to different cooling rates, since the high hardenability of the alloys contributes to the same microstructure of the entire weld metal. However, small deviations in cooling rates cause significant

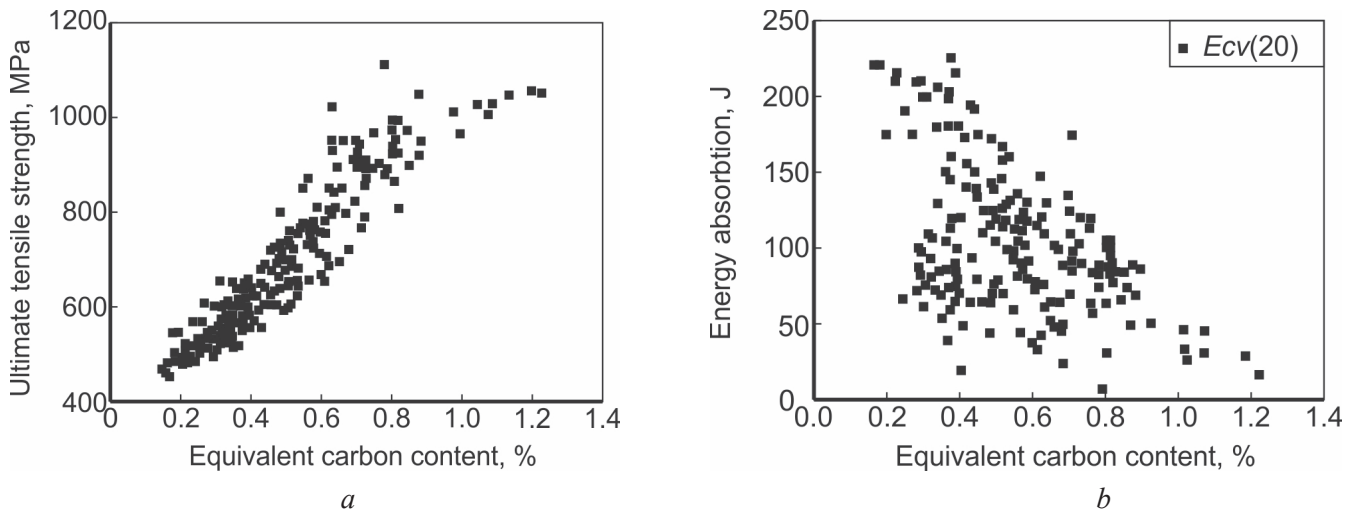


Fig. 1. The effect of the carbon equivalent on the ultimate tensile strength (a) and impact strength at 20 °C of weld metals (b) [32]

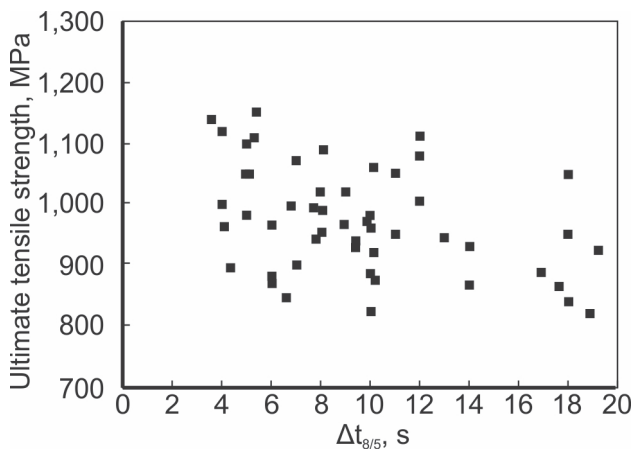


Fig. 2. The effect of weld metal cooling rate ($\Delta t_{8/5}$) on the ultimate tensile strength of high-strength pipeline steels [4]

changes in the amount of martensite, bainite and acicular ferrite [30]. Figure 2 shows that a high scatter band is observed when high-strength weld metals are cooled for different times in the temperature range 800–500 °C [4].

Standards [5–10] allow a wider range of alloying and micro-alloying elements, and therefore each manufacturer offers its own chemistry to achieve qualification requirements. Carbon equivalent (C_{eq}) was included in the standard [5] because it is generally related to hardenability.

Limits for C_{eq} were calculated based on the minimum and maximum alloying element contents. Therefore, a lower C_{eq} value is always preferable, indicating good weldability. The *American Petroleum Institute* has adopted two formulas (CE_{IIW} and $CE P_{cm}$) [5] to determine the carbon equivalent limit for *API PSL 2*

pipe steel. The CE_{IIW} formula is provided by the *International Welding Institute* and is commonly used for carbon and carbon-manganese steels. In Europe P_{cm} is the critical parameter of the metal. $CE P_{cm}$ is taken from the documents of the *Japan Society of Welding Engineers*. $CE P_{cm}$ was proposed specifically for testing the weldability of high-strength steels. The balance of superior strength and toughness can be disrupted following thermal cycling that occurs during welding, causing poor toughness in the heat-affected zone (HAZ) [11–19].

General welding issues

Modern steels with high strength and high impact toughness are widely used in pipelines, shipbuilding and various manufacturing industries [2, 3]. Changes in steel production technology and the steel rolling process pose a challenge to the production of welding consumables and joining technology. It is important to note that, in contrast to the production of wrought steel, the strength and toughness of weld metals, as a rule, should be achieved through alloying [2–4]. As a consequence, due to the complexity of welding processes and the limitation of heat input and, consequently, cooling rates, the toughness of the weld metal at low temperatures is lower than that of the base metal [3, 4]. In addition [2–4], the microstructure of weld metals with a yield strength of 600 MPa and above consists mainly of bainite and martensite, rather than predominantly acicular ferrite. Therefore, the calculation of the basic composition of the weld metal should

be different for each case [2]. In fact, for those applications where the strength of the weld metal consisting of acicular ferrite is insufficient, it is necessary to add special strengthening elements for solid solution and other alloying elements to retard the austenite/ferrite transformation and produce martensitic welds with the required high strength.

In work [4], specimens obtained by the *SMAW* (*Submerged Metal Arc Welding*) method were studied; automatic submerged metal arc welding and *GMAW* (*Gas Metal Arc Welding*) is a designation used to indicate the use of the *MIG/MAG* method in automatic (robotic) welding. The authors wanted to evaluate (figure 3) whether the use of the *GMAW* process could improve the weld performance of high-strength steels while maintaining good quality even at lower levels of reheat. It was found that a good relationship between mechanical strength and toughness could be obtained.

Multi-pass welding is widely used in pipe manufacturing, circular welding of pipe butt joints, and in-service welding. For automatic welding of large diameter pipes, the root welding method by an internal welding machine and the cap welding of external welding machine are usually used [18]. The pipe neck group is first welded to the inner root of the pipeline using a welding robot, and then the weld root is welded (hot pass), then the filler and lining layers of the joint are welded, as shown in figure 4, where layer 0 is a root weld, layers 1–6 are filling ones, and layers 7–8 are cap ones. The first layer completes the fusion of the root weld. Due to the large number of filling layers, the likelihood of defects greatly increases.

Thermal cycles encountered during welding are characterized by a range of peak temperatures that can alter the microstructure and properties of the *HAZ* compared to the base metal. It was found that the supercritical (reheated above A_{c3}) and subcritical (reheated below A_{c1}) regions resulting from the second thermal cycle retain toughness properties comparable to the original ones.

Among all the sub-zones of the *HAZ* in multi-pass welding, the *IC-CGHAZ* (i.e., the pre-existing *CGHAZ* reheated to the temperature range between A_{c1} and A_{c3} in a subsequent weld) is considered to be subject to the most significant degradation in toughness [11–18]. This is confirmed by the work of the authors [29,

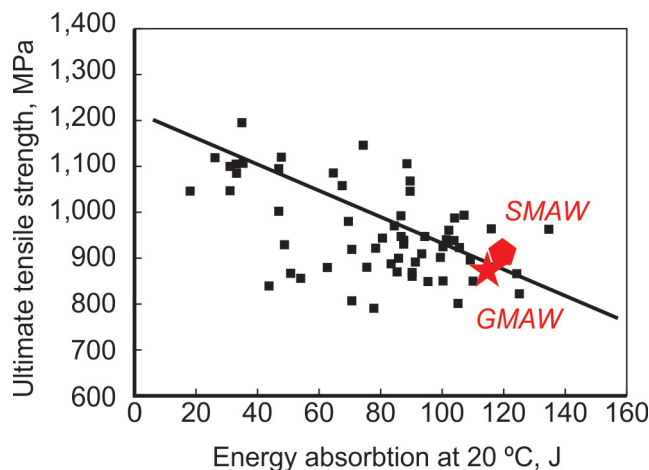


Fig. 3. The relationship between the mechanical strength and impact toughness of the weld deposit of high strength steels in comparison with several works by *SMAW* (*Submerged Metal Arc Welding*) and *GMAW* (*Gas Metal Arc Welding*) method [4]

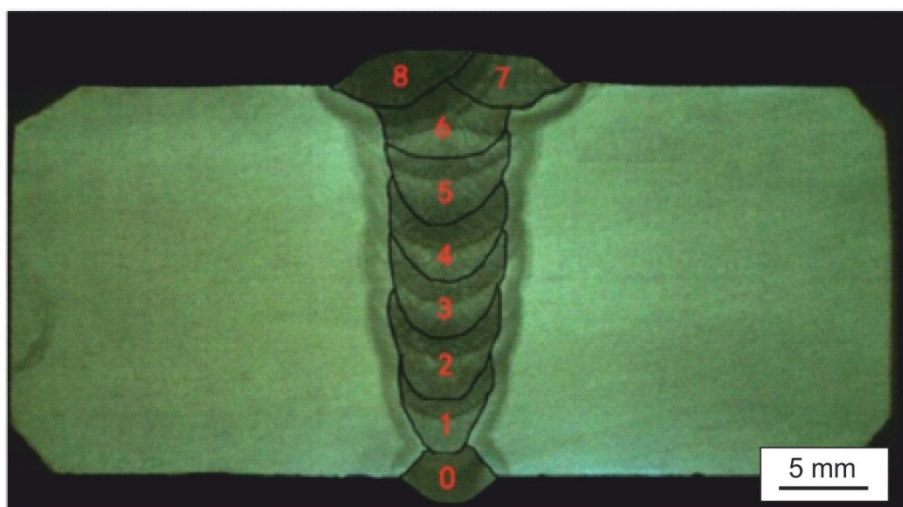


Fig. 4. Transverse microsection of an annular welded joint of pipes with narrow edge cutting [18]

30], and the significant deterioration of *IC-CGHAZ* is associated with the presence of a blocky component of the martensite-austenite grain boundary (*M-A*).

It is well known that the *HAZ* is the weakest part of the welded joint and determines the safety of pipeline operation. In particular, the lowest impact toughness was obtained in the coarse-grained microstructure of the *HAZ* [16–19], which is adjacent to the fusion line of the weld.

Low impact toughness of the *HAZ* at low temperatures is the main problem limiting the use of high-quality steels for pipelines [2–4, 11–29].

Description of microstructures

It should be recognized that the problems of welding high-strength steels are far from being solved. For example, it is known that non-metallic inclusions formed in the cast weld metal have two opposite effects on impact strength [30]. Firstly, inclusions act as initiation sites for both ductile and shear fractures [29–31], and secondly, it can promote the formation of acicular ferrite, which is recognized as the most optimal microstructure [31–42].

One of the basic requirements for pipeline joints is to obtain weld metal of equal or higher strength than the base material to avoid localized deformation or failure of the weld under load. However, sufficient strength is also required, which is usually verified using *Charpy* impact tests. A common solution is to develop the weld metal to produce acicular ferrite (*AF*) in the metal structure, which provides a balance between strength and toughness [28, 29]. This fact has stimulated extensive research into the mechanisms of *AF* formation in weld metals and the determination of what factors control its formation [11–39].

The key factor in the formation of *AF* is the chemical composition of the consumable welding wire, both from the point of view of the isolated effect of each element and the combined effect of the general composition [29–38].

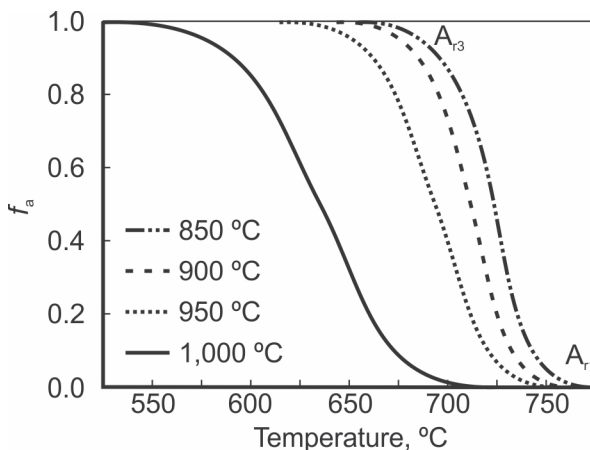


Fig. 5. The fractions of phase transformation determined by dilatometric measurements as a function of temperature during continuous cooling in X65 pipeline steel specimens austenitized at different temperatures from 850 °C to 1,000 °C [30]

In a review [32] on the formation of acicular ferrite in carbon-manganese surfacing, it was reported that the following elements influence the formation of acicular ferrite: *C*, *Mn*, *Si*, *Ni*, *Ti*, *Al*, *Mo* and *Nb*.

The effect of austenitization temperature in the range of 850–1,000 °C on acicular ferritic transformation in *Cr65 HSLA* pipeline steel was investigated [31]. As shown in figure 5, the initial and final phase transformation temperatures during continuous cooling, namely A_{r1} and A_{r3} , respectively, decreased with increasing austenitization temperature. This result suggests that increasing austenitization improves the stability of austenite during cooling and thus delays the decomposition of austenite. The decomposition products of austenite in *Cr65* steel consist mainly of polygonal ferrite, pearlite, acicular ferrite, etc. [30]. Increasing the austenitization temperature promotes the formation of acicular ferrite and prevents the formation of pearlite and polygonal ferrite (see figure 6).

A higher austenitization temperature leads to more sufficient dissolution of carbide-forming elements such as *Nb*, *V* and *Ti*, as well as more sufficient homogenization in the austenite [30]. The authors of [31] believe that dissolved alloy elements improve the stability of metastable austenite. Thus, according to the authors, the decomposition of austenite is delayed to a lower temperature, which is also confirmed by fig. 3. As a diffusionless reaction [32], the acicular ferrite transformation is more likely to occur at a relatively low temperature than the diffusion-controlled pearlite or polygonal ferrite transformation [33], since the rate of atomic diffusion decreases with decreasing temperature.

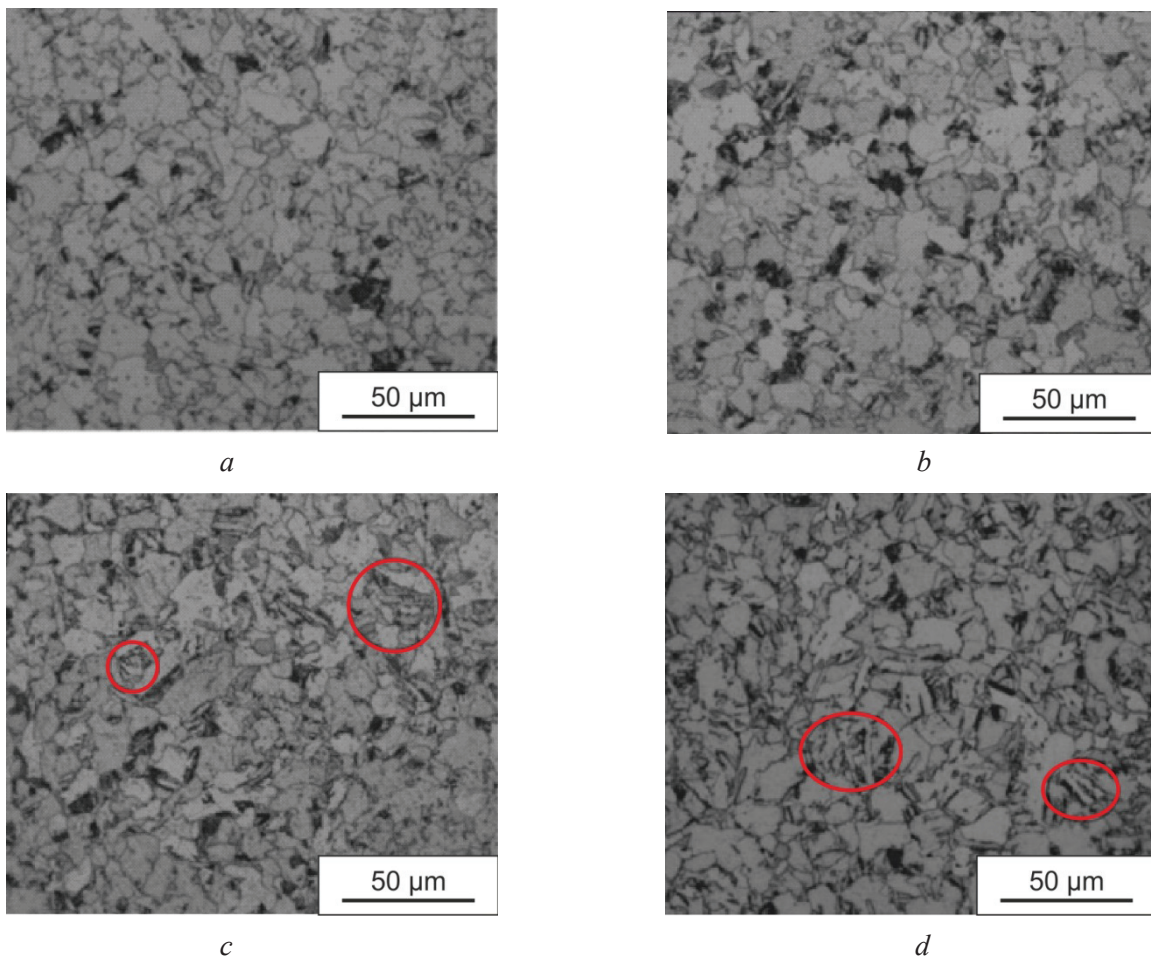


Fig. 6. Optical micrographs of X65 pipeline steel specimens after continuous cooling with different austenitization temperatures:
850 °C (a), 900 °C (b), 950 °C (c) and 1,000 °C (d) [30]

Copper has been reported to contribute to the formation of *AF* when using manual arc welding [32]. Many elements will combine with the oxygen present in the weld metal, which can be controlled by shielding gas and/or the composition of the weld metal. The oxygen reaction influences *AF* formation by either promoting or inhibiting the formation of nonmetallic inclusions such as oxides.

Some authors argue [29–48] that oxides act as nucleation sites for *AF*, so an increase in oxygen content favors the formation of *AF*. For example, it was reported [33, 34] that increasing oxygen content to 300 ppm changed the weld metal of *Widmanstätten* side plates to *AF* microstructure [33, 34].

The formation of *AF* is also facilitated by coarse austenite grains with a large number of inclusions with a diameter of more than 0.2 μm. The details of the formation of *AF* are now well described as a variant of the bainite structure in numerous works by *Bhadeshia* and his students [48], where it is shown that it is a special variant that depends on intragranular formation [33]. Thus, it is necessary to achieve sufficient preliminary austenite grain size and number density of non-metallic inclusions of favorable chemical composition, especially based on titanium oxides. However, it has also been noted in many works that if the amount of non-metallic inclusions reaches a certain level depending on the oxygen content, it has a detrimental effect on the toughness as the crack initiation sites outweigh the benefits of achieving a fine *AF* structure.

Two welding materials suitable for joining *Cr80* steel pipes are compared in terms of weld metal microstructure, hardness, toughness and tensile properties [35]. The chemical composition of the consumables was similar: one of the consumables had a rich chemical composition of the wire and contained higher alloying additives *C*, *Ni*, *Ti* compared to the depleted wire. Deposit welding was performed using a gas arc welding (*GMAW*) process system to achieve the same heat input of 0.66 kJ/mm. The results showed that for both wires, the microstructure of the weld metal was mainly composed of acicular ferrite.

Consumables with a richer chemical composition (*C*, *Ni* and *Ti*) showed higher strength and hardness due to the finer microstructure of the final weld metal; however, *Charpy* impact test results showed that the depleted chemical wire had higher impact strength at low temperature. Since both weld metals had a similar acicular ferrite structure, the lower toughness of the richer weld was attributed to the presence of titanium inclusions, which could become crack initiation sites.

The effect of welding method and preheating on the weld metals of pipeline steels was investigated in the work of *HSLA* steel. It is known that post-welding treatment reduces the strength characteristics of the metal of the welded joint [2, 4]. The results of studies [4] assessing the preheating up to 200 °C and welding treatment of welded joints showed a tendency towards a decrease in mechanical strength and an increase in impact strength as a consequence of some important aspects, such as a lower percentage of martensite, coarsening of the microstructure and a higher proportion of high-angle boundaries (> 15 %). Longer cooling times (time spent in the temperature range of 800–500 °C) show a tendency to improve the impact toughness and reduce the mechanical strength of deposited metals in high-strength steels.

Microstructure features affecting the impact strength of weld metals

Multi-pass welding is required to connect the main pipes. This leads to overheating of the *HAZ*. This creates its own peculiarities of thermal effects on the metal and, as a result, non-classical phase and structural transformations with sharp temperature and stress gradients. The *HAZ* zone can be divided into coarse-grained *HAZ* (*CGHAZ*), fine-grained *HAZ* (*FGHAZ*), intercritical *HAZ* (*ICHAZ*) and subcritical *HAZ* (*SCHAZ*), when a single thermal cycle is applied to weld the material [43].

When a second weld bead is applied over an existing one, it results in the formation of a plurality of reheated *HAZ* structures that are characterized by corresponding second peak temperatures and include supercritical, intercritical and subcritical structures. The strength and toughness of *HSLA* pipeline steel can degrade significantly after one or two welding thermal cycles, so *CGHAZ* with intercritical reheating (*ICR*) are often considered to be the weakest link or most fragile area of the weld joint. A schematic representation of a weld with different heat-affected zones is shown in figure 7 [38].

Various metallurgical factors such as austenite grain size and bainite stack size, as well as the size, shape and distribution of any second phase (carbide or martensitic-austenitic) can influence fracture toughness. In particular, the presence of so-called martensitic-austenitic (*MA*) constituents formed in *ICR CGHAZ* plays a decisive role in the fracture toughness at low temperatures.

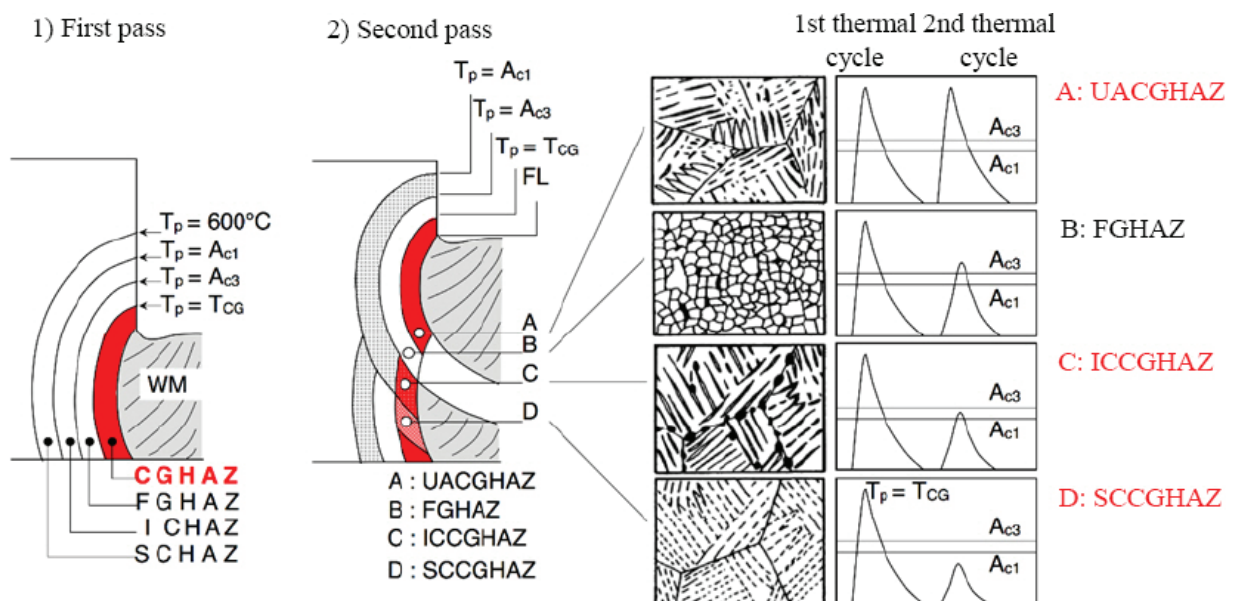


Fig. 7. Schematic representation of microstructures in the heat-affected zone of multi-pass welds [43]

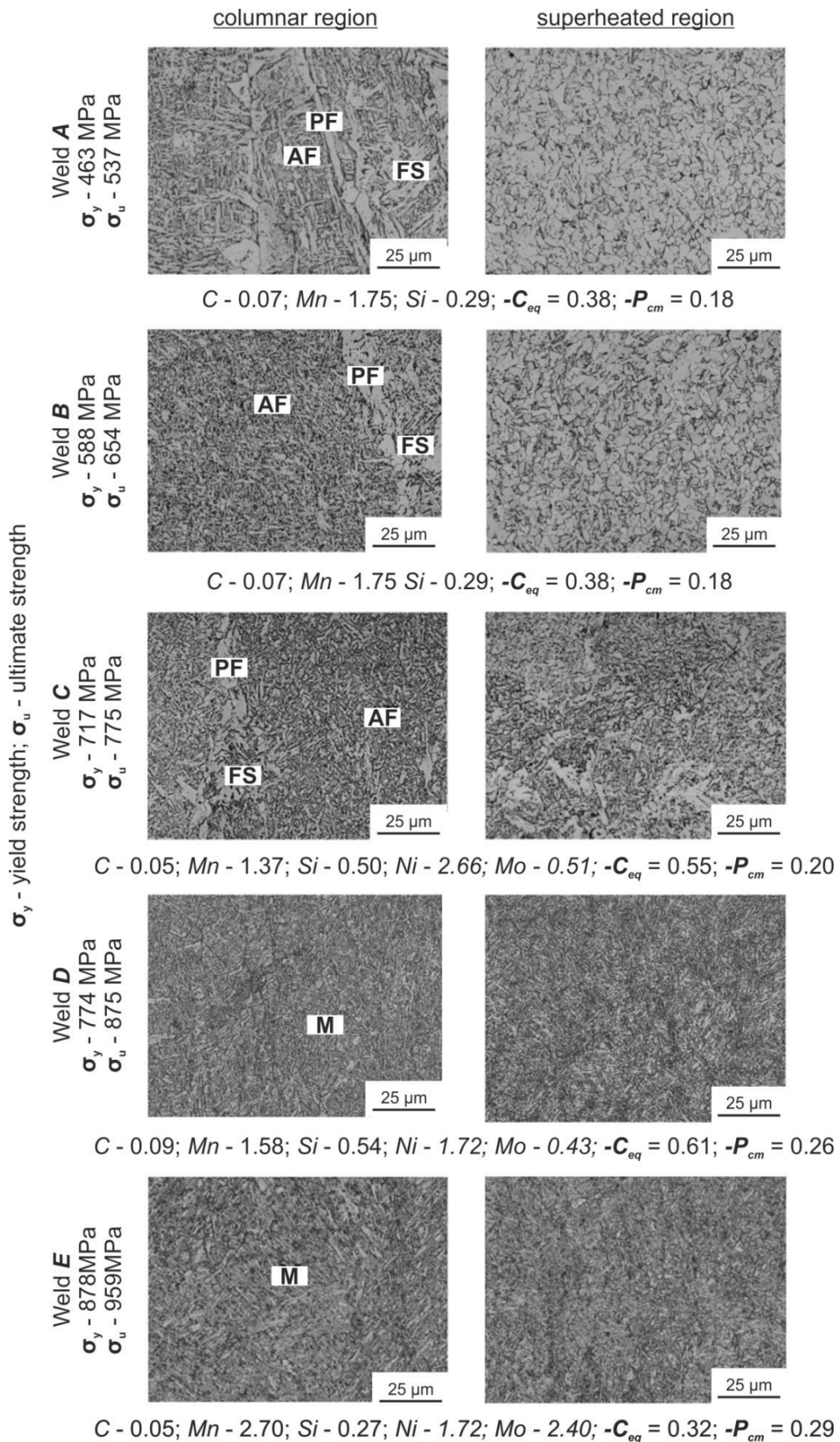
Although *MA* has been widely studied in recent decades, the effect of cooling rate on its volume fraction remains controversial [23–29]. Some researchers have shown that increasing the cooling rate increases the *MA* fraction, while others have shown, on the contrary, [32–35] that a slower cooling rate decreases the *MA* fraction. Works [38–48] showed that for various steels there is an increase in the fraction of *MA* at a lower cooling rate. In addition to the effect of cooling rate on *MA* fraction, the effect of *MA* grain size, morphology and distribution on impact toughness has also not been established. This is largely due to the complex factors that determine impact strength, including the fraction, size, substructure and morphology of *MA*. It is generally accepted that *MA* reduces the impact strength of pipeline steel [4]. A slower cooling rate results in a coarser *MA* structure, resulting in poor toughness properties. In the work [43] it is reported that the formation of lath type (thin *MA*), associated with poor toughness, occurs at slower cooling rates, while block *MA* is formed at higher cooling rates. It is important for further analysis to interpret the microstructure of steel after welding because this is controversial because constituents that are part of the same primary structure may appear morphologically different depending on the viewing plane (figs. 8, 9), and some structures may have similar morphological features but present different mechanical properties [44–46]. Fig. 7 shows an overview of the evolution of the major components present in the weld metal as observed by optical microscopy (*OM*). This figure shows that the microstructure changes continuously with increasing carbon equivalent (C_{eq}). A mixture of acicular ferrite (*AF*), primary ferrite (*PF*) and ferrite with a second phase (*FS*) in the columnar region has lower strength values. In contrast, the reheat region is dominated by polygonal ferrite. In addition to the tendency to have a mixture of martensite and bainite with a higher content of alloying elements due to increased hardenability, it is worth noting the presence of similar components for both columnar and reheated areas.

The terminology of microstructural constituents observed in weld metals has been very confusing [35], with different terms being used to refer to the same constituent. This lack of clarity prompted the *International Institute of Welding (IIW)* to develop a general framework for microstructure quantification [36] in the 1980s, where components were easily identified using optical microscopy (*OM*).

Another critical issue relates to the low resolution of optical microscopy for refining the constituents of refined weld metals, even when using higher magnification than recommended by the *IIW* [38, 39]. To solve this problem, scanning electron microscopy (*SEM*) has been widely used in recent decades, mainly to separate bainite and martensite and evaluate micro-phases. However, sometimes even this method has limitations in distinguishing the overall microstructure. This occurs mainly for weld metals with a tensile strength greater than 600 MPa, where a mixed microstructure consisting of acicular ferrite, bainite (ferrite with a second phase) and martensite predominates.

To ensure proper resolution in the study of microstructure, the *EBS*D technique is used as an additional tool [11, 12, 32]. This method has been considered as an interesting alternative [32–40] to overcome the shortcomings of optical microscopy. This method, which provides valuable grain boundary information, is useful for refined microstructures to confirm constituents such as acicular ferrite, bainite and martensite. The high clarity provided by *EBS*D, especially at grain boundaries, is useful for separating acicular ferrite and bainite (second-phase ferrite). Regarding the assessment of *MA* components and inclusions, *SEM* analysis is more suitable for this task [36–39]. Thus, it is believed [11, 12, 24, 25, 32–40] that a combination of *OM*, *SEM* and *EBS*D methods provides the best methodology for the study of metal welds in *C-Mn* steel in the presence of a refined microstructure.

In [38], the author examined the *IIW* scheme for the main structures that develop during reduction and shear transformation in steels. However, he noted that questions remain to be resolved regarding reaction kinetics, especially elucidating the growth mechanisms of bainite, which could lead to greater precision in distinguishing bainite from other phases. In [38], a critical review is presented to clarify the existing confusion in the literature regarding bainite and acicular ferrite due to the similarity in appearance of these two microstructural constituents observed under an optical microscope. The works [44–48] present a description of the microstructural components in relation to low-carbon pipe steels.



σ_y - yield strength; σ_u - ultimate strength

Fig. 8. Microstructures observed in weld metals with increase in tensile strength after etching with Nital 2%. Magnification: 1,000× (OM). Where:

AF – acicular ferrite; PF – primary ferrite; FS – second phase ferrite; M – martensite [32]

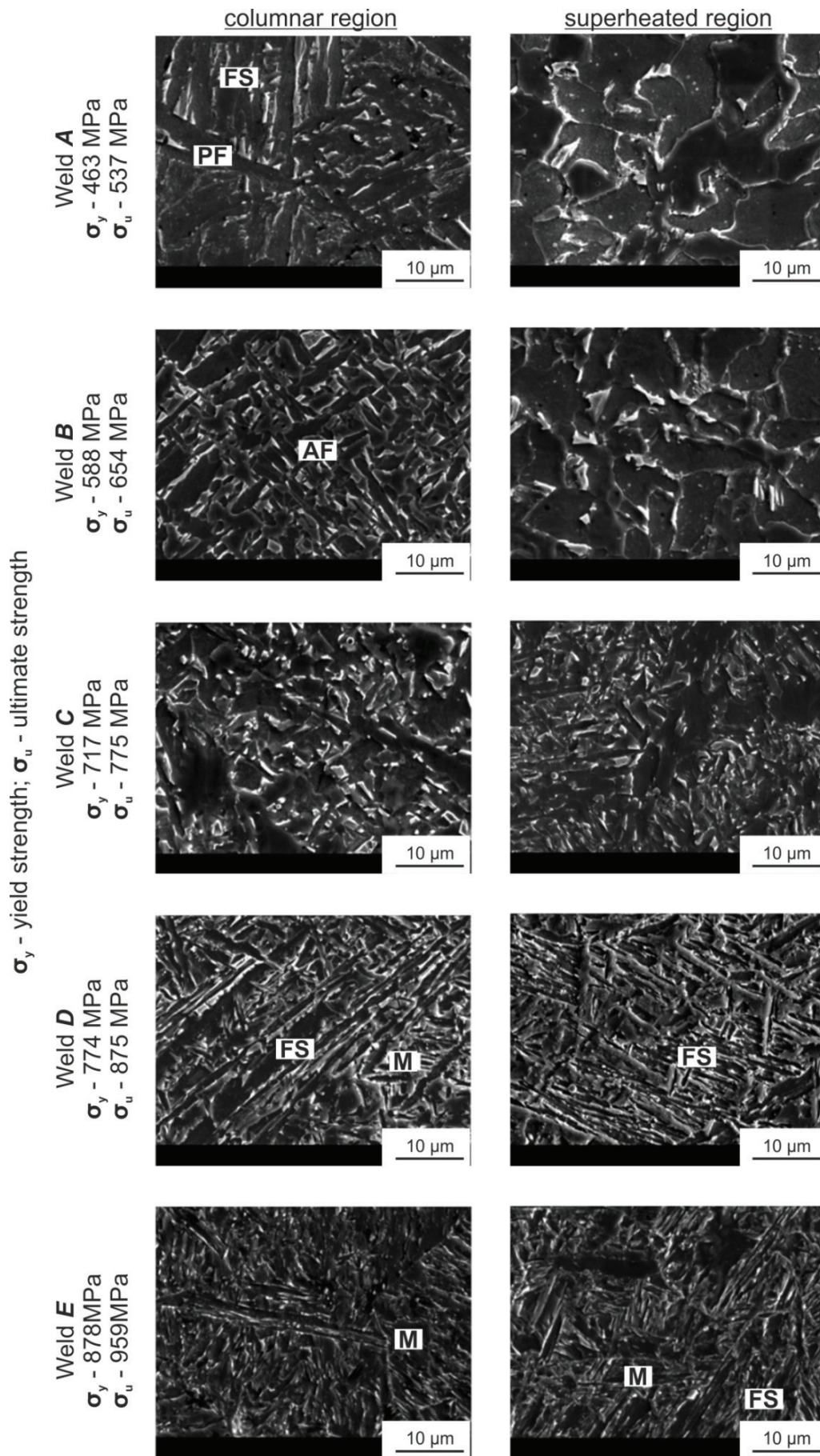


Fig. 9. SEM images of weld metals are shown after etching with *Nital* 2 %. Where: AF – acicular ferrite; PF – primary ferrite; FS – ferrite with second phase; M – martensite [32]

Our analysis shows that, in relation to low-carbon pipe steels, the weld metal can have the following microstructures [11–49]:

- primary ferrite, which is nucleated at the boundaries of the initial austenite grains (allotriomorphic ferrite) and to a lesser extent inside the austenite grains (euhedral ferrite), where non-metallic inclusions (*NI*) are presented [39–42]. Primary ferrite with nuclei at grain boundaries is formed during cooling in the temperature range of 1,000 and 650 °C [20–34];

- side plates of ferrite [34, 39–42] (separated by low-angle boundaries) are formed during cooling at temperatures from 750 to 650 °C, also at the boundaries of primary austenite grains [29];

- acicular ferrite [34, 39–42] is heterogeneously nucleated on the surface of non-metallic inclusions during the austenite-ferrite transition. As the transformation proceeds, ferrite grains diverge in different directions, creating a chaotic structure [29, 30] of crystallographically misoriented plates approximately 5–15 µm long and 1–3 µm wide [17–29, 39–42]. The temperature range, over which acicular ferrite is formed, depends on the overall composition and cooling rate across the transformation temperature range, but is typically in the range of 750–560 °C [34, 35].

- bainite grows in the form of individual plates or subunits [48], which can form bundles of parallel ferrite laths [34]. It can be classified as upper or lower bainite depending on the transformation temperature. In upper bainite, carbon is deposited as cementite (Fe_3C) between bainitic ferrite plates (bundles) [48]. In lower bainite, the ferrite becomes supersaturated with carbon, and some carbide precipitation occurs within the ferrite subunits as well as between it [43]. The initial temperature of bainite depends on the composition and cooling rate, but is usually on the order of 560 °C [48–67]. The nucleation efficiency of nonmetallic inclusions in modern low-alloy steel weld metals is such that the colony size of intragranular bainite is similar to the size of acicular ferrite in *C-Mn* steel weld metal [29]. Consequently, when examined under an optical microscope, the colonies within granular bainite are very similar to the type of acicular ferrite with which it is confused in the literature [41–44]. Some authors [44, 45] use the term granular bainite, which does not differ from lath bainite in terms of the transformation mechanism, although granular bainite packets form at relatively higher temperatures and mainly consist of wide parallel laths, while lath bainite packets form at relatively lower temperatures and consist of thin parallel slats;

- transformation of pearlite can occur at the boundaries of austenite grains or in such inhomogeneities as inclusions. At high transformation temperatures, pearlite forms nodules of alternating plates of ferrite and cementite, which can be quite large. As the transformation temperature decreases, the pearlite sheets become increasingly thinner until the structure becomes indistinguishable under a light microscope. Alternatively, distorted pearlite plates may appear as a virtually indistinguishable ferrite/carbide aggregate [53–56]. Lamellar pearlite, $FC(P)$ in the IIW classification scheme [35], can be confused with martensite if the ferrite/cement laminae are indistinguishable under the optical microscope [2, 41–44].

- martensite is formed as a result of a rapid and diffusion-free transformation, in which carbon remains in solution [43]. Martensite can occur in the form of laths or plates. The substructure of lath martensite is characterized by a high density of dislocations located in cells, where each martensite plate consists of many dislocation cells. The substructure of lamellar martensite consists of very small twins, i.e. twinned martensite [42–45].

The mechanisms of formation of the components are not discussed in this work, since there is extensive material on this topic in the literature [33–67].

It is noted in [67] that, unlike metals of single-pass welds, metals of multi-pass welds contain in each bead (except for the last bead) a large proportion of overheated areas, which, due to subsequent beads, are reheated to a temperature above A_{c3} .

The effect of multiple welding passes on *C-Mn* and low-alloy steel deposits is very complex since the proportion of columnar and recrystallized regions and its corresponding microstructures depend on various parameters such as heat input, temperature between passes and chemical composition [29]. The previous columnar morphology changes during the reheating process, resulting in a heterogeneous microstructure that affects the performance of the welded joint [4, 29, 32].

Mechanical properties

The authors [4] stated that only a few studies have examined the mechanical properties of reheated weld metals. The results are still inconsistent as it depends on several factors such as the amount of acicular ferrite and the presence of *MA* components. The authors of [29–33] noted that understanding the variation in toughness in the multi-pass weld metal of *C-Mn* steels is very difficult, even if the effect of reheating due to multiple passes is taken into account. Similarly, the authors of [29, 38–42] suggested that significant changes in the toughness of *C-Mn* weld metals are due to the microstructural features existing in the *Charpy-V* notch, which are the combined result of the chemical composition, welding procedure, deposition sequence and specific welding methods.

In addition to the factors mentioned above, it is critical to consider the position of the *Charpy-V* notch in relation to the proportion of weld metal reheated. A specific assessment should be made for each case. The author [48] observed that although complete recrystallization was observed for two intersecting regions per layer and the proportion of reheated regions was about 75–80 % for three layers, the same toughness was obtained for both sequences, depending on the *Mn* content.

In general, toughness increases when the fraction of recrystallized region increases due to the predominance of polygonal ferrite, microstructure refinement, or tempering effects during subsequent deposition [41–58, 67]. However, some data suggests that this property deteriorates with extensive segregation [29, 30] or the presence of micro-phases located along the grain boundaries of the previous austenite [47, 48]. Another negative contribution is associated with a decrease in the proportion of acicular ferrite due to the smaller size of the precursor equiaxed austenite grains in the reheated weld metal [46–53].

Figure 10 shows an *OM* image of a *Charpy-V* notch, where the ratio of columnar and reheated regions can be easily determined for *C-Mn* weld metals since these regions are well defined. For more alloyed weld metals, this distinction can be more complex. In this case, several polishing and etching steps may be required to enhance the contrast between the areas.

The authors of [54] noted that only a few studies have focused on the microstructure and toughness of actual weld metal. This is because it is very difficult to analyze its correlation using a real weldment, and the precise determination of the correlation between the ring-type *MA* component in the weld metal reheat zone and the toughness is still uncertain.

At the same time, after metallographic studies, when an accurate characterization of the microstructure has been obtained, it is possible to assess impact strength based on the following criteria.

(1) *Reheat*. This criterion is less representative in many of the studies analyzed because the same proportion of recrystallization was obtained for all deposits;

(2) *Microstructure*. *EBS*D results confirm this trend, showing that finer microstructure has a higher frequency of high-angle boundaries (*HABs*), which can effectively cause the propagation of cleavage cracks to deflect or stop [32–46]. The same behavior was noted for the reheating region of the refined grains, where polygonal ferrite predominates;

(3) *No metallic inclusions*. It is known that non-metallic inclusions can have two opposite effects on impact toughness [11, 12]. One of it is that inclusions act as crack initiation sites, both plastic and cleavage. Secondly, it can promote the formation of acicular ferrite. It has been observed that increasing the *Ti* content promotes the formation of inclusions sufficient to support the formation of purified acicular ferrite, in agreement with other works [3, 11, 12, 32, 36].

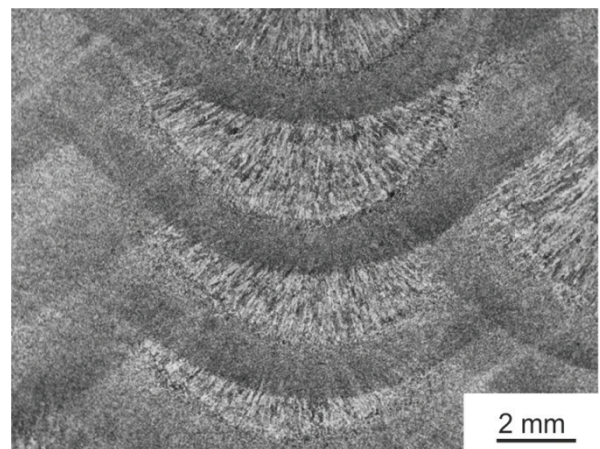


Fig. 10. Optical microscopy at low magnification of the *Charpy-V* notch position for *C-Mn* weld metal after etching with *Nital 2 %* [32]

The proposed methodology for the proper description of the microstructure to explain the impact toughness of weld metals is as follows:

– The mechanical properties of weld metals are a consequence of the microstructure, mainly related to its alloying elements and the cooling rate. Regardless of the chemistry, for decades a cooling time from 800 to 500 °C ($\Delta t_{8/5}$) has been used as a guideline for achieving desired welding performance and, in certain cases, a limited interval is recommended to ensure superior performance. For example, in some works a range of 5–20 s is recommended for high-strength weld metals [4, 17, 29–31].

– Although $\Delta t_{8/5}$ does not take into account any microstructural transformations such as lower bainite formed at temperatures below 500 °C, the author [48] notes that this indicator can be used for high-strength steels because it refers not only to the time spent on cooling in the temperature range of 800–500 °C, but also to the entire thermal cycle, including the time spent at high temperatures. Usually, in order to achieve the recommended maximum value of $\Delta t_{8/5}$, the welding energy input is limited, which leads to a decrease in the deposition rate of the weld metal and the need for a greater number of welding passes [4].

In general, longer cooling times due to higher heat inputs result in a coarser microstructure [38–57] and ultimately the presence of undesirable components such as granular bainite, fused bainite, or aggregate ferrite-carbides [48]. Although decomposition of *MA* components can improve mechanical properties, replacement with large carbides does not necessarily provide positive results [45–50].

To overcome these problems, suppliers can change the basic composition of welding consumables; this is because welding consumable standards allow a wider range of alloying and micro-alloying elements, and therefore each manufacturer offers its own chemistry to achieve qualification requirements.

Conclusion

In accordance with the purpose of this work and the objective of the review study, our analysis of numerous studies shows that for pipe steel weld metal, acicular ferrite (*AF*) is the most desirable component due to its fine grain size and interlocking structure with high-angle boundaries, providing high impact toughness [39–46].

It has also been reported [46–48] that *AF* is the weld metal component that best improves the toughness of *HSLA* steels with a yield strength of about 600 MPa. The structure with smaller grains has more boundaries and changes the direction of crack propagation, acting as effective barriers since it has different crystallographic orientations [46–48]. Therefore, in recent decades, much work has been aimed at identifying the factors that control the formation of acicular ferrite [43–52]. According to the study [47, 52], conducted using electron backscatter diffraction analysis [48–51], polygonal ferrite also acts as a strengthening phase because its boundaries are high-angle ones and there is a relatively low dislocation density within the grains.

As mentioned, a large amount of acicular ferrite is critical to the toughness of weld metals. Weld metal with a significant amount of acicular ferrite can more effectively control other important parameters such as inclusions and *MA* components. This is because acicular ferrite refines the microstructure, which improves the size and distribution of *MA*, which determines the level of brittleness caused by *MA* [18]. In addition, a large amount of acicular ferrite, which is favored by small inclusions, minimizes the harmful effects of inclusions acting as initiation sites for both ductile and cleavage failures [28–44].

The combination of good toughness with a high proportion of acicular ferrite in the top bead of weld deposits is not the most suitable solution, even in single-pass welding [37–43]. In this regard, it is important to emphasize the position of the *Charpy-V* notch relative to the appearance of columnar deposited or reheated weld metal [43–53]. Moreover, it is necessary to take into account the influence of inclusions, which is directly related to the results of *Charpy-V* tests at higher temperatures. This situation may be different for higher strength levels of steel, since the microstructure is dominated by bainite and martensite rather than acicular ferrite, and its relative amount and morphology are critical to toughness. Even if the microstructure is more uniform in both the columnar and heated regions, multiple welding passes are also relevant due to recrystallization. Clearly, all of these factors contribute to the results obtained from *Charpy-V* tests and make its analysis significantly more complex than that associated with tensile tests.

Based on the data presented in this work, all microstructural aspects shown previously should be taken into account when performing a complete toughness analysis. Thus, an appropriate methodology for characterizing microstructure to explain treatment outcomes should include an analysis of all contributing factors. However, its relative importance varies for each weld metal and experimental procedure.

The authors of this paper believe that the methodology described in the steps shown below is suitable for assessing the toughness of weld metals. The *Charpy-V* notch in all tests should be located in the area of interest to the researcher of the specimen.

Step 1. Measure the proportion of columnar and reheated regions due to recrystallization effects using low magnification optical microscopy. However, this is not applicable to single pass weld metals;

Step 2. Qualitative and quantitative analysis of the main microstructural constituents, namely primary ferrite, acicular ferrite, polygonal ferrite, second phase ferrite and martensite, using optical microscopy (1,000× magnification). However, for stronger weld metals containing a mixture of acicular ferrite, second-phase ferrite, and martensite, *SEM* analysis is sometimes necessary to clarify the major constituents (~1,000–3,000× magnification). In addition, the *EBSD* method can be used as a complementary one. In this case, useful results include effective grain size (*EGS*) and high-angle boundary (*HAB*) frequency obtained from grain boundary disorientation profiles;

Step 3. Qualitative and quantitative analysis of micro-phases, carbides and components of *MA* using *SEM* (~ 2,000–5,000× magnification). Although some studies claim that *EBSD* is an excellent method to confirm the presence of *MA* components, it is important to remember that statistical results depend on the number of points measured, and in this regard, quantitative analysis using *SEM* is easier and faster. The authors of this paper believe that the software available for *EBSD* is still not reliable enough for this task due to its complexity.

Step 4. Qualitative and quantitative analysis of non-metallic inclusions using *SEM/EDS* (~1,500× magnification). This analysis is useful for higher energy levels and when comparing different welding processes. In addition, this may confirm the potential of inclusions as acicular ferrite nuclei.

There are more detailed studies in the literature, the full analysis of which is not required. Using all the steps above involves more complex analysis. Our analysis of various sources of information on the assessment of various microstructures of *C-Mn* and high-strength steels welds and the establishment of the relationship between microstructure and impact strength based on experimental results obtained over the past decades for metals of welds with tensile strength from 400 to 1,000 MPa allowed formulate conclusions for further research on this topic.

Summary

1. It is shown that high-strength low-alloy (*HSLA*) steels have a good combination of strength, toughness and weldability and are widely used in long-distance oil and gas transportation systems [2–4]. Pipeline steels *Cr80*, 100, 120 are produced using thermo-mechanical control process (*TMCP*) followed by accelerated cooling to achieve excellent mechanical properties. An important consideration when preparing pipeline welds is to achieve equal or higher strength and toughness of the weld metal compared to the base metal to avoid failure of the weld metal.

2. Based on an analysis of experimental data from various authors, it is shown that it is extremely important to have an optimal microstructure of the weld metal, which largely depends on the composition of the electrode wire. Major alloying elements such as *Cu*, *Ni* and *Mo*, as well as micro-alloying elements such as *V*, *Nb*, *Ti* and *B*, are widely used to optimize the microstructure and properties of pipeline steels.

3. The predominant microstructure of acicular ferrite (*AF*) with *MA* islands as the second phase is shown to be the optimal microstructure for pipeline steel weld metal. Extensive research into the mechanisms of acicular ferrite formation in weld metals shows that elements such as *C*, *Mn*, *Si*, *Ni*, *Al*, *Ti*, *Nb* and *Mo* influence the nucleation of acicular ferrite within austenite grains. The effect of *Ti* addition on the microstructure and formation of inclusions in steel pipeline joints welded by automatic submerged arc welding showed that the best combination of microstructure and toughness can be obtained by adding *Ti* in

the range of 0.02–0.05 wt. %. The improvement in toughness with increasing titanium content is due to the greater amount of acicular ferrite, as other factors do not interfere.

Adding *Mo* in an amount of 0.881 wt. % in the weld metal provides optimal toughness at –45 °C due to a microstructure consisting of 77 % acicular ferrite and 20 % granular bainite.

4. It is necessary to take into account the overall chemical composition of the welding wire, which significantly affects the formation of acicular ferrite (*AF*). It is shown that the best mechanical properties in welds of *Cr70* steels corresponded to two compositions of electrode wires, i.e. 1.92 wt. % *Mn* with 0.02 wt. % *Ti* and 1.40 wt. % *Mn* with 0.08 wt. % *Ti*. A further increase in the *Ti* or *Mn* content contributed to the nucleation of bainite at the grain boundaries, rather than intra-granular nucleation of acicular ferrite. Therefore, a satisfactory combination of strength and toughness depends on the control of the composition of the weld metal.

5. An important factor determining the microstructure of the weld is the cooling rate, which is usually defined as the time required for cooling from 800 to 500 °C ($\Delta t_{8/5}$) [34–36]. As shown in numerous works by various authors, the cooling rate depends on the heat input during welding. Therefore, it makes sense in further work to study the evolution of the microstructure of the weld metal at various heat inputs.

6. It is shown that the manufacture or repair of steel pipelines with a relatively large section thickness, as a rule, requires multi-pass welding. Numerous works extensively studied the brittleness of the heat-affected zone (*HAZ*) caused by thermal cycles from successive thermal welding cycles. Similarly, weld metals are subjected to thermal cycling from subsequent welding passes. The effect of uneven reheating causes a non-uniform microstructure of the welds. In this regard, in the course of further research, it is very important to understand the influence of thermal cycles of welding on the microstructure of the weld metal during multi-pass welding performed by various methods.

References

1. Karlina Yu.I., Kononenko R.V., Ivancivsky V.V., Popov M.A., Deriugin F.F., Byankin V.E. Obzor sovremennykh trebovaniy k svarke trubnykh vysokoprochnykh nizkolegirovannykh staley [Review of modern requirements for welding of pipe high-strength low-alloy steels]. *Obrabotka metallov (tekhnologiya, oborudovanie, instrumenty) = Metal Working and Material Science*, 2023, vol. 25, no. 4, pp. 36–60. DOI: 10.17212/1994-6309-2023-25.4-36-60.
2. Efron L.I. *Metallovedenie v «bol'shoi» metallurgii. Trubnye stali* [Metallurgy in “big” metallurgy. Pipe steels]. Moscow, Metallurgizdat Publ., 2012. 696 p. ISBN 978-5-902194-63-7.
3. Matrosov Yu.I., Litvinenko S.A., Golovanenko S.A. *Stal' dlya magistral'nykh truboprovodov* [Steel for main pipelines]. Moscow, Metallurgiya Publ., 1989. 288 p.
4. Jorge J.C.F., Monteiro J.L.D., Gomes A.J.C., Bott I.S., Souza L.F.G., Mendes M.C., Araújo L.S. Influence of welding procedure and PWHT on HSLA steel weld metals. *Journal of Materials Research and Technology*, 2019, vol. 8 (1), pp. 561–571. DOI: 10.1016/j.jmrt.2018.05.007.
5. API Spec 5CT. *Obsadnye i nasosno-kompressornye truby. Tekhnicheskie usloviya* [API Spec 5CT. Casing and tubing. Specifications]. 9th ed. American Petroleum Institute Publ., 2011. 287 p.
6. ISO 11960. *Petroleum and natural gas industries – Steel pipes for use as casing or tubing for wells*. 4th ed. International Organization for Standardization, 2011. 269 p.
7. DSTU ISO 11960:2020. *Petroleum and natural gas industries – Steel pipes for use as casing and tubing for wells*. Geneva, Switzerland, IOS, 2020.
8. GOST R 53366–2009. *Truby stal'nye, primenyaemye v kachestve obsadnykh ili nasosno-kompressornykh trub dlya skvazhin v neftyanoi i gazovoi promyshlennosti. Obshchie tekhnicheskie usloviya* [State Standard R 53366–2009. Steel pipes for use as casing or tubing for wells in petroleum and natural gas industries. General specifications]. Moscow, Standardinform Publ., 2010. 190 p.
9. STO Gazprom 2-4.1-158–2007. *Tekhnicheskie trebovaniya k obsadnym trubam dlya mestorozhdenii OAO «Gazprom»* [Standard organization STO Gazprom 2-4.1-158–2007. Technical requirements for casing pipes for Gazprom fields]. Moscow, Gazprom Publ., 2007. 23 p.
10. STO Gazprom 2-4.1-228–2008. *Tekhnicheskie trebovaniya k nasosno-kompressornym trubam dlya mestorozhdenii OAO «Gazprom»* [Standard organization STO Gazprom 2-4.1-228–2008. Technical requirements for tubing for OAO Gazprom fields]. Moscow, Gazprom Publ., 2008. 32 p.



11. Heisterkamp F., Hulka K., Matrosov Yu.I., Morozov Y.D., Efron L.I., Stolyarov V.I., Chevskaya O.N. *Niobii-soderzhashchie nizkolegirovannye stali* [Niobium containing low alloy steels]. Moscow, Internet Engineering Publ., 1999. 94 p.
12. Baker T.N. Microalloyed steels. *Ironmaking & Steelmaking*, 2016, vol. 43 (4), pp. 264–307. DOI: 10.1179/1743281215Y.0000000063.
13. Baker T.N. Titanium microalloyed steels. *Ironmaking & Steelmaking*, 2019, vol. 46 (1), pp. 1–55. DOI: 10.1080/03019233.2018.1446496.
14. Pickering F.B. Overview of titanium microalloyed steels. *Titanium technology in microalloyed steels*. Ed. by T.N. Baker. London, The Institute of Materials, 1997, p. 10–43.
15. Morrison W.B. Microalloy steels – the beginning. *Materials Science and Technology*, 2009, vol. 25 (9), pp. 1066–1073. DOI: 10.1179/174328409X453299.
16. Morrison W.B. Influence of small niobium additions on properties of carbon-manganese steels. *Journal of the Iron and Steel Institute*, 1963, vol. 201 (4), pp. 317–325.
17. Midawi A.R.H., Santos E.B.F., Huda N., Sinha A.K., Lazor R., Gerlich A.P. Microstructures and mechanical properties in two X80 weld metals produced using similar heat input. *Journal of Materials Processing Technology*, 2015, vol. 226, pp. 272–279. DOI: 10.1016/j.jmatprotec.2015.07.019.
18. Sha Q., Li D. Microstructure, mechanical properties and hydrogen induced cracking susceptibility of X80 pipeline steel with reduced Mn content. *Materials Science and Engineering: A*, 2013, vol. 585, pp. 214–221. DOI: 10.1016/j.msea.2013.07.055.
19. Zhang H., Zhang H., Lu C.H. Fracture toughness and application of X80 pipeline steel. *Materials Science Forum*, 2019, vol. 944, pp. 938–943. DOI: 10.4028/www.scientific.net/MSF.944.938.
20. Yin T., Wang J., Zhao H., Zhou L., Xue Z., Wang H. Research on filling strategy of pipeline multi-layer welding for compound narrow gap groove. *Materials*, 2022, vol. 15, p. 5967. DOI: 10.3390/ma15175967.
21. Li B., Luo M., Yang Z., Yang F., Liu H., Tang H., Zhang Z., Zhang J. Microstructure evolution of the semi-macro segregation induced banded structure in high strength oil tubes during quenching and tempering treatments. *Materials*, 2019, vol. 12 (20), p. 3310. DOI: 10.3390/ma12203310.
22. Balanovskiy A.E., Astafyeva N.A., Kondratyev V.V., Karlina A.I. Study of mechanical properties of C-Mn-Si composition metal after wire-arc additive manufacturing (WAAM). *CIS Iron and Steel Review*, 2021, vol. 22, pp. 66–71. DOI: 10.17580/cisirs.2021.02.12.
23. Shtayger M.G., Balanovskiy A.E., Kargapoltsev S.K., Gozbenko V.E., Karlina A.I., Karlina Yu.I., Govorkov A.S., Kuznetsov B.O. Investigation of macro and micro structures of compounds of high-strength rails implemented by contact butt welding using burning-off. *IOP Conference Series: Materials Science and Engineering*, 2019, vol. 560 (1), p. 012190. DOI: 10.1088/1757-899X/560/1/012190.
24. Balanovskiy A.E., Astafyeva N.A., Kondratyev V.V., Karlina Yu.I. Study of impact strength of C-Mn-Si composition metal after wire-arc additive manufacturing (WAAM). *CIS Iron and Steel Review*, 2022, vol. 24, pp. 67–73. DOI: 10.17580/cisirs.2022.02.10.
25. Balanovsky A.E., Shtayger M.G., Kondrat'ev V.V., Karlina A.I., Govorkov A.S. Comparative analysis of structural state of welded joints rails using method of Barkhausen effect and ultrasound. *Journal of Physics: Conference Series*, 2018, vol. 1118 (1), p. 012006. DOI: 10.1088/1742-6596/1118/1/012006.
26. Zhang Q., Yuan Q., Xiong Z., Liu M., Xu G. Effects of Q&T parameters on phase transformation, microstructure, precipitation and mechanical properties in an oil casing steel. *Physics of Metals and Metallography*, 2021, vol. 122 (14), pp. 1463–1472. DOI: 10.1134/S0031918X21140180.
27. Kim Y.M., Kim S.K., Lim Y.J., Kim N.J. Effect of microstructure on the yield ratio and low temperature toughness of linepipe steels. *ISIJ International*, 2002, vol. 42 (12), pp. 1571–1577. DOI: 10.2355/isijinternational.42.1571.
28. Kolosov A.D., Gozbenko V.E., Shtayger M.G., Kargapoltsev S.K., Balanovskiy A.E., Karlina A.I., Sivtsov A.V., Nebogin S.A. Comparative evaluation of austenite grain in high-strength rail steel during welding, thermal processing and plasma surface hardening. *IOP Conference Series: Materials Science and Engineering*, 2019, vol. 560, p. 012185. DOI: 10.1088/1757-899X/560/1/012185.
29. Balanovskii A.E., Vu Van Huy. Estimation of wear resistance of plasma-carburized steel surface in conditions of abrasive wear. *Journal of Friction and Wear*, 2018, vol. 39 (4), pp. 311–318. DOI: 10.3103/S1068366618040025.
30. Balanovskii A., Vu Van Huy. Plasma surface carburizing with graphite paste. *Letters on Materials*, 2017, vol. 7 (2), pp. 175–179. DOI: 10.22226/2410-3535-2017-2-175-179.
31. Balanovskiy A.E., Shtayger M.G., Kondratyev V.V., Karlina A.I. Determination of rail steel structural elements via the method of atomic force microscopy. *CIS Iron and Steel Review*, 2022, vol. 23, pp. 86–91. DOI: 10.17580/cisirs.2022.01.16.



32. Jorge J.C.F., Souza L.F.G. de, Mendes M.C., Bott I.S., Araújo L.S., Santos V.R. dos, Rebello J.M.A., Evans G.M. Microstructure characterization and its relationship with impact toughness of C–Mn and high strength low alloy steel weld metals – a review. *Journal of Materials Research and Technology*, 2021, vol. 10, pp. 471–501. DOI: 10.1016/j.jmrt.2020.12.006.
33. Zhukov I.A., Martyushev N.V., Zyukin D.A., Azimov A.M., Karlina A.I. Modification of hydraulic hammers used in repair of metallurgical units. *Metallurgist*, 2022, vol. 65 (11–12), pp. 1644–1652. DOI: 10.1007/s11015-023-01480-w.
34. Shao Y., Liu C., Yan Z., Li H., Liu Y. Formation mechanism and control methods of acicular ferrite in HSLA steels: a review. *Journal of Materials Science & Technology*, 2018, vol. 34 (5), pp. 737–744.
35. Babu S.S. The mechanism of acicular ferrite in weld deposits. *Current Opinion in Solid State and Materials Science*, 2004, vol. 8 (3–4), pp. 267–278. DOI: 10.1016/j.cossms.2004.10.001.
36. Beidokhti B., Kokabi A.H., Dolati A. A comprehensive study on the microstructure of high strength low alloy pipeline welds. *Journal of Alloys and Compounds*, 2014, vol. 597, pp. 142–147. DOI: 10.1016/j.jallcom.2014.01.212.
37. Dong H., Hao X., Deng D. Effect of welding heat input on microstructure and mechanical properties of HSLA steel joint. *Metallography Microstructure and Analysis*, 2014, vol. 3, pp. 138–146. DOI: 10.1007/s13632-014-0130-z.
38. Thewlis G. Classification and quantification of microstructures in steels. *Materials Science and Technology*, 2004, vol. 20 (2), pp. 143–160. DOI: 10.1179/026708304225010325.
39. Dolby R.E. Guidelines for the classification of ferritic steel weld metal microstructural constituents using the light microscope. *Welding in the World*, 1986, vol. 24 (7), pp. 144–149.
40. Ramirez J.E. Examining the mechanical properties of high-strength steel weld metals. *Welding Journal*, 2009, vol. 88 (1), pp. 32–38.
41. Lan L., Kong X., Qiu C., Zhao D. Influence of microstructural aspects on impact toughness of multi-pass submerged arc welded HSLA steel joints. *Materials and Design*, 2016, vol. 90, pp. 488–498. DOI: 10.1016/j.matdes.2015.10.158.
42. Zhou P., Wang B., Wang L., Hu Y., Zhou L. Effect of welding heat input on grain boundary evolution and toughness properties in CGHAZ of X90 pipeline steel. *Materials Science and Engineering: A*, 2018, vol. 722, pp. 112–121. DOI: 10.1016/j.msea.2018.03.029.
43. Matsuda F., Fukada Y., Okada H., Shiga C., Ikeuchi K., Horii Y., Shiwaku T., Suzuki S. Review of mechanical and metallurgical investigations of martensite-austenite constituent in welded joints in Japan. *Welding in the World/Le Soudage dans le Monde*, 1996, vol. 3 (37), pp. 134–154.
44. Luo X., Chen X., Wang T., Pan S., Wang Z. Effect of morphologies of martensite-austenite constituents on impact toughness in intercritically reheated coarse-grained heat-affected zone of HSLA steel. *Materials Science and Engineering: A*, 2018, vol. 710, pp. 192–199. DOI: 10.1016/j.msea.2017.10.079.
45. Abson D.J. Acicular ferrite and bainite in C–Mn and low-alloy steel arc weld metals. *Science and Technology of Welding and Joining*, 2018, vol. 23 (8), pp. 635–648. DOI: 10.1080/13621718.2018.1461992.
46. An G., Park J., Ohata M., Minami F. Evaluation of fracture safety according to plastic deformation with high strength steel weld joints. *Journal of Welding and Joining*, 2019, vol. 37 (6), pp. 547–554. DOI: 10.5781/JWJ.2019.37.6.3.
47. Smirnov M.A., Pyshmintsev I.Yu. Boryakova A.N. Classification of low-carbon pipe steel microstructures. *Metallurgist*, 2010, vol. 54 (7–8), pp. 444–454. DOI: 10.1007/s11015-010-9321-2. Translated from *Metallurg*, 2010, no. 7, pp. 45–51.
48. Pyshmintsev I.Yu., Mal'tseva A.N., Smirnov M.A. Rol' strukturnykh sostavlyayushchikh v formirovanii svoistv sovremennykh vysokoprochnykh stalei dlya magistral'nykh truboprovodov [The role of structural components in the formation of properties of modern high-strength steels for main pipelines]. *Nauka i tekhnika v gazovoi promyshlennosti = Science and Technology in the Gas Industry*, 2011, no. 4, pp. 46–52.
49. Pyshmintsev I.Yu., Gervas'ev A.M., Mal'tseva A.N., Struin A.O. Osobennosti mikrostruktury i tekstury trub K65 (Kh80), vliyayushchie na sposobnost' materiala trubyy ostanavlivat' protyazhennoe vyazkoe razrushenie [Features of microstructure and texture of K65 (X80) pipes influencing the ability of the pipe material to stop the extended ductile fracture]. *Nauka i tekhnika v gazovoi promyshlennosti = Science and Technology in the Gas Industry*, 2011, no. 4, pp. 73–78.
50. Smirnov M.A., Pyshmintsev I.Yu., Mal'tseva A.N., Mushina O.V. Vliyanie ferritno-beinitnoi struktury na svoistva vysokoprochnoi trubnoi stali [Effect of ferrite-bainite microstructure on characteristics of high-strength pipe steel]. *Metallurg = Metallurgist*, 2012, no. 1, pp. 55–62. (In Russian).
51. Bhadeshia H.K.D.H. *Bainite in steels: theory and practice*. 3rd ed. London, CRC Press, 2015. 616 p. DOI: 10.1201/9781315096674.



52. Zhao H., Wynne B.P., Palmiere E.J. A phase quantification method based on EBSD data for a continuously cooled microalloyed steel. *Materials Characterization*, 2017, vol. 123, pp. 339–348. DOI: 10.1016/j.matchar.2016.11.024.
53. Strateichuk D.M., Martyushev N.V., Klyuev R.V., Gladkikh V.A., Kukartsev V.V., Tynchenko Y.A., Karlina A.I. Morphological features of polycrystalline CdS_{1-x}Se_x films obtained by screen-printing method. *Crystals*, 2023, vol. 13 (5), p. 825. DOI: 10.3390/cryst13050825.
54. Bosikov I.I., Martyushev N.V., Klyuev R.V., Tynchenko V.S., Kukartsev V.A., Ereemeeva S.V., Karlina A.I. Complex assessment of X-ray diffraction in crystals with face-centered silicon carbide lattice. *Crystals*, 2023, vol. 13 (3), p. 528. DOI: 10.3390/cryst13030528.
55. De-Castro D., Eres-Castellanos A., Vivas J., Caballero F.G., San-Martín D., Capdevila C. Morphological and crystallographic features of granular and lath-like bainite in a low carbon microalloyed steel. *Materials Characterization*, 2022, vol. 184, p. 111703. DOI: 10.1016/j.matchar.2021.111703.
56. Zhao H., Wynne B.P., Palmiere E.J. Conditions for the occurrence of acicular ferrite transformation in HSLA steels. *Journal of Materials Science*, 2018, vol. 53, pp. 3785–3804. DOI: 10.1007/s10853-017-1781-3.
57. Ramirez J.E. Characterization of high-strength steel weld metals: chemical composition, microstructure, and nonmetallic inclusions. *Welding Journal*, 2008, vol. 87 (3), pp. 65s–75s.
58. Lan L., Chang Z., Kong X., Qiu C., Zhao D. Phase transformation, microstructure, and mechanical properties of X100 pipeline steels based on TMCP and HTP concepts. *Journal of Materials Science*, 2017, vol. 52, pp. 1661–1678. DOI: 10.1007/s10853-016-0459-6.
59. Lan L., Qiu C., Zhao D., Gao X. Microstructural evolution and mechanical properties of Nb-Ti microalloyed pipeline steel. *Journal of Iron and Steel Research International*, 2011, vol. 18 (2), pp. 57–63. DOI: 10.1016/S1006-706X(11)60024-1.
60. Chu Q., Xu S., Tong X., Li J., Zhang M., Yan F., Zhang W., Bi Z., Yan C. Comparative study of microstructure and mechanical properties of X80 SAW welds prepared using different wires and heat inputs. *Journal of Materials Engineering and Performance*, 2020, vol. 29, pp. 4322–4338. DOI: 10.1007/s11665-020-04986-5.
61. Beidokhti B., Koukabi A.H., Dolati A. Effect of titanium addition on the microstructure and inclusion formation in submerged arc welded HSLA pipeline steel. *Journal of Materials Processing Technology*, 2009, vol. 209, pp. 4027–4035. DOI: 10.1016/j.jmatprotec.2008.09.021.
62. Bhole S.D., Nemade J.B., Collins L., Liu C. Effect of nickel and molybdenum additions on weld metal toughness in a submerged arc welded HSLA line-pipe steel. *Journal of Materials Processing Technology*, 2006, vol. 173, pp. 92–100. DOI: 10.1016/j.jmatprotec.2005.10.028.
63. Rezanov V.A., Martyushev N.V., Kukartsev V.V., Tynchenko V.S., Kukartsev V.A., Grinek A.V., Skeebe V.Y., Lyosin A.V., Karlina A.I. Study of melting methods by electric resistance welding of rails. *Metals*, 2022, vol. 12 (12), p. 2135. DOI: 10.3390/met12122135.
64. Mamadaliev R.A., Bakhmatov P.V., Martyushev N.V., Skeebe V.Yu., Karlina A.I. Influence of welding regimes on structure and properties of steel 12KH18N10T weld metal in different spatial positions. *Metallurgist*, 2022, vol. 65 (11–112), pp. 1255–1264. DOI: 10.1007/s11015-022-01271-9.
65. Malushin N.N., Gizatulin R.A., Martyushev N.V., Valuev D.V., Karlina A.I., Kovalev A.P. Strengthening of metallurgical equipment parts by plasma surfacing in nitrogen atmosphere. *Metallurgist*, 2022, vol. 65 (11–112), pp. 1468–1475. DOI: 10.1007/s11015-022-01292-4.
66. Yelemessov K., Baskanbayeva D., Martyushev N.V., Skeebe V.Y., Gozbenko V.E., Karlina A.I. Change in the properties of rail steels during operation and reutilization of rails. *Metals*, 2023, vol. 13, p. 1043. DOI: 10.3390/met13061043.
67. Beidokhti B., Koukabi A.H., Dolati A. Influence of titanium and manganese on high strength low alloy SAW weld metal properties. *Materials Characterization*, 2009, vol. 60, pp. 225–233. DOI: 10.1016/j.matchar.2008.09.005.

Conflicts of Interest

The authors declare no conflict of interest.

© 2024 The Authors. Published by Novosibirsk State Technical University. This is an open access article under the CC BY license (<http://creativecommons.org/licenses/by/4.0>).

